

Ultrafast Excitation of Molecular Adsorbates on Flash-Heated Gold Surfaces

Jeffrey A. Carter, Zhaohui Wang, Hiroki Fujiwara, and Dana D. Klott*

School of Chemical Sciences, University of Illinois at Urbana–Champaign, Chemical and Life Sciences Laboratory, 600 South Mathews Avenue, Urbana, Illinois 61801

Received: June 29, 2009; Revised Manuscript Received: September 17, 2009

An ultrafast flash-thermal conductance technique is used to study energy transfer from a flash-heated polycrystalline Au(111) surface to adsorbed thiolate self-assembled monolayers (SAMs). The focus is on understanding energy transfer processes to parts of SAM molecules situated within a few carbon atoms of the Au surface, by probing specific SAM functional groups with vibrational sum-frequency generation (SFG) spectroscopy. The SFG intensity drop after flash-heating for benzenethiol (BT) CH-stretch transitions shows a substantial overshoot lasting several tens of picoseconds before BT and Au equilibrate at a higher temperature estimated at 600 °C. The thermal redshift of BT CH-stretch transitions also shows an overshoot. Other aromatic molecules and aliphatic molecules such as cyclohexanethiol (CHT) and hexanethiol (C6) have an overshoot as well. A model is proposed where the overshoot is primarily the result of hot surface electrons existing only during the flash-heating pulses. The intensity overshoot is caused by electron excitation of the probed vibrations and the redshift overshoot is caused by electron excitation of lower-energy vibrations anharmonically coupled to the probed vibration. Although electron excitation causes a substantial perturbation, up to 50% in some cases, of the SFG signal, the total amount of energy deposited into SAMs by electrons is much smaller than the heat transferred by Au surface phonons. Studies of a variety of molecular structures including substituted benzenes, biphenyl and terphenyl, and benzene rings connected to the Au surface by alkane linkers show that the likelihood of electron excitation becomes small for distances of 4–5 carbon atoms above the surface.

1. Introduction

In this paper, we describe measurements using an ultrafast molecular flash-thermal conductance technique developed recently,^{1,2} of energy transfer from polycrystalline Au(111) surfaces flash-heated by femtosecond laser pulses to estimated temperatures of 600 °C, to self-assembled monolayers (SAMs) of aryl and alkyl thiol adsorbates. In previous works,^{1,2} our group used this technique to study heat flow along even-numbered alkanethiolate SAMs from C6 to C24, ranging in length from 1.2 to 3.5 nm. As illustrated in Figure 1a, we showed that vibrational sum-frequency generation spectroscopy (SFG) of CH-stretch transitions of the alkane terminal methyl groups could be used as a molecular thermometer^{1,2} to measure heat flow from the Au surface, along the alkane chains, to the terminal methyl groups. The SFG thermometer had a thickness comparable to the ~ 1.5 Å diameter of the terminal methyl groups and a response time of < 1 ps.^{1,2} As shown in Figure 1b, the SFG signal from terminal methyl groups decreased after flash heating to ~ 800 °C.^{1,2} Molecular simulations² indicated that such heating caused the initially well-aligned methyl groups to become thermally disordered, which reduced the coherent SFG emission intensity. Figure 1b shows how the SFG signal from $\nu_s(\text{CH}_3)$ of C16 chains (2880 cm^{-1}) lost intensity after flash heating. The small peak near $t = 0$ is an artifact that functions as a fiducial marker.^{2,3}

Because alkanes shorter than C6 were not stable enough for those measurements, which involved many thousands of high-intensity laser pulses, we could not directly probe the details of energy transfer from the metal surface to moieties that were separated from the surface by fewer than six carbon atoms.

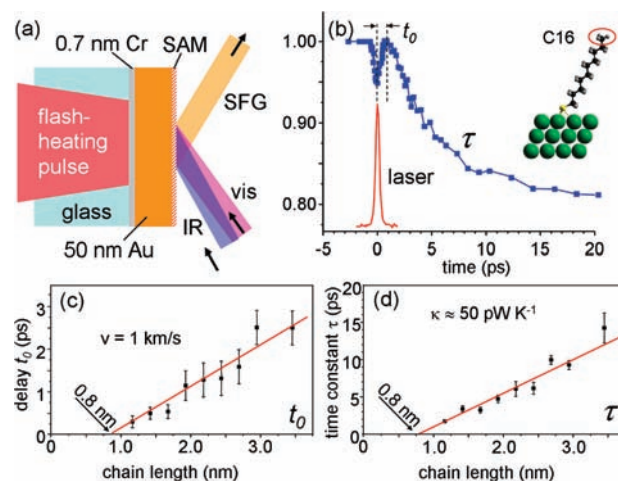


Figure 1. (a) Ultrafast flash-thermal conductance method. A femtosecond pulse flash-heats the back side of Au to create a T-jump of ~ 600 K. Vibrational sum-frequency generation (SFG) probes vibrational transitions of a self-assembled monolayer (SAM) on the back side. (b) Response of hexadecylthiolate SAM to flash-heating. SFG probes the intensity of the symmetric CH-stretch transition of the terminal methyl groups. There is an artifact at $t = 0$ used as a fiducial marker. The SFG intensity loss is characterized by an onset delay time t_0 and an exponential time constant τ . (c,d) Chain-length dependence of t_0 and τ . Both sets of data intersect the x axis at 0.8 nm, which suggests that energy transfer from Au to SAM is instantaneous for chains 4–5 carbon atoms or less in length. Adapted from ref 2 copyright AAAS.

However, we did make a very interesting observation² about the short-chain-length behavior illustrated in Figure 1c,d. The time response of the SFG thermometer from all alkane chains

* Corresponding author.

in the C6–C24 range had the same characteristic shape as the data shown in Figure 1b for the C16 chains. This shape was characterized by two parameters t_0 and τ . The t_0 parameter was the delay time before the thermometer first began to respond, and τ was the time constant characterizing the exponential rise to the final temperature. Both t_0 and τ were observed to increase linearly with chain length.² We interpreted t_0 as the time for the initial heat burst to propagate along the alkane chains, from the Au surface to the terminal methyl groups. The linear length dependence indicated that the heat burst propagated ballistically, and the results yielded a velocity of 1 km/s. The linear length dependence of τ indicated that the rate of chain heating was directly proportional to the chain heat capacity, which increases linearly with chain length. This type of dependence occurs when heat flow is dominated by a thermal barrier at the Au–SAM interface.^{1,4} In such cases, heat flow across the interface is the same for all chains, but longer chains need more heat to attain the final temperature.

Figure 1c,d has x axis intercepts that are not zero but instead 0.8 nm, which corresponds to a chain with 4–5 carbon atoms. Of course this intercept is an extrapolated quantity, but if we take Figure 1c,d literally, they would say that chains 4–5 carbon atoms or less in length are heated instantaneously by the Au surface. This result is consistent with theory from Nitzan's group,^{5–7} who found that the heat-carrying vibrations of short-chain alkanes are delocalized over \sim 4–5 carbon segments. We concluded that phonons of the Au surface couple to and transmit energy to a "base region" of the alkane chains 4–5 carbon atoms in length.^{1,2} This interesting observation is the motivation for the present study, which examines a variety of molecules that probe energy transfer processes at close distances from a flash-heated Au surface.

As illustrated by Figure 1c,d, our measurement technique provides a real-time monitor of heat flow along alkane chains and across mismatched metal–organic interfaces.⁸ For the Au–alkanethiol system, we measured a value for the interface thermal conductance of $G = 220(\pm 100)$ MW m⁻² K⁻¹.² Prior measurement techniques were able to measure interface thermal conductances but did not have the ability to measure energy flow through the SAM molecules. Those measurements involved a sandwich arrangement where a SAM was the filling between two bulk media. Ge et al. measured heat flow from an Au surface through an AT SAM out to an aqueous medium^{9,10} and obtained $G = 100$ – 300 MW m⁻² K⁻¹. Wang et al.¹¹ studied steady-state heat flow across a Au–AT–GaAs structure and obtained a much smaller value of $G = 25$ MW m⁻² K⁻¹. In the former two measurements, there is one significantly mismatched Au–AT interface and a SAM/water interface that should be a good match. In the latter measurement, there are two significantly mismatched interfaces, Au–AT and AT–GaAs.

In follow-up studies to our alkanethiol work, we first looked at SAMs made from benzenethiol (BT),^{1,3} whose height above the surface is about the same as a C4 chain. With benzenethiol (BT), we obtained the unexpected results shown in Figure 2,^{1,3} where we used SFG to probe the phenyl CH-stretch transition at 3070 cm⁻¹. (The data in Figure 2 are new results from an improved apparatus.) After the T-jump, both the SFG intensity drop and the peak shift show an overshoot relative to the longer time values when Au and BT are assuredly in thermal equilibrium. The peak shift overshoot is much smaller than the intensity drop overshoot. The intensity overshoot clearly stems from the very fast intensity drop near $t = 0$, that has a 10%–90% risetime of 0.4 ps. Such dramatic and rapid SFG intensity changes were never observed in the alkane chain experiments.

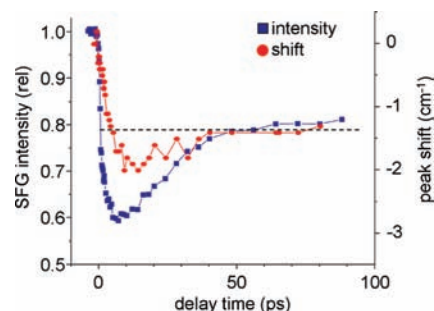


Figure 2. SFG intensity loss from benzenethiolate (BT) SAM on Au after flash heating to \sim 600 °C shows a significant overshoot from the longer-time equilibrium value. The intensity overshoot is associated with the very fast intensity drop occurring in the first \sim 600 fs, which is not seen in longer-chain alkanethiols. The peak redshift shows a smaller overshoot.

We cannot imagine any way of putting in contact a hotter and a colder object and having the temperature of the colder object temporarily exceed the temperature of the hotter object by a significant amount. So this data indicates that, while the SFG signal from BT at longer times >30 ps is a good molecular thermometer, during the overshoot period, SFG is not a good thermometer. The SFG signal must be reporting at least one additional process. In a previous paper,¹ we made a tentative suggestion that the overshoot resulted from a combination of the thermometer effect plus a contribution from a SAM structural relaxation process. Now that we have repeated these experiments with much better accuracy and have studied a number of other SAM structures, we propose a different interpretation: excited electrons generated in Au during the flash-heating pulse directly excite SAM vibrations. Excitation of the higher-energy vibration being probed and excitation of lower-energy vibrations anharmonically coupled to the probed vibration (both of which are temporarily in excess of their ultimate thermal populations) are responsible for the intensity drop overshoot and peak shift overshoot, respectively.

In this study, we first present new time-resolved reflectance data to better characterize the metal surface T-jump. In our previous work, we characterized surfaces with only a small T-jump of \sim 10 K. These new results involve the same flash-heating conditions as the SAM experiments, where $\Delta T \approx 600$ K. We then present flash-heating data on SAMs comprised of the molecules shown in Figure 3. There are three classes of SAMs, short alkanes, methyl, nitro, and phenyl-substituted benzenes, and benzene-linker molecules of the form $(C_6H_5)-(CH_2)_n-SH$ ($n = 0$ – 5) denoted BT, B1T, B2T, and so forth.

2. Experimental Section

A. Samples. The details of sample preparation were described in previous papers.^{1–3,12} The samples consisted of $50 \times 50 \times 1.6$ mm³ glass substrates vacuum coated with 0.8 nm Cr and 50 nm Au. The SAMs were grown by overnight soaking of the substrates in thiol solution followed by several rinses with ethanol and water. All of the SAMs were deposited from ethanol solution except BPhT and TPhT which were poorly soluble in ethanol. For these SAMs, we used an ethanol–benzene mixture (BPhT) or cyclohexanol (TPhT) to improve solubility.

The origins and acronyms of the molecules depicted in Figure 3 are as follows. 4-nitrobenzenethiol (NBT), 2-methylbenzenethiol (2MBT), hexanethiol (C6), cyclohexanethiol (CHT), benzenethiol (BT), benzylthiol (B1T), and phenylethylthiol (B2T) were purchased from Aldrich Chemical Co. and used

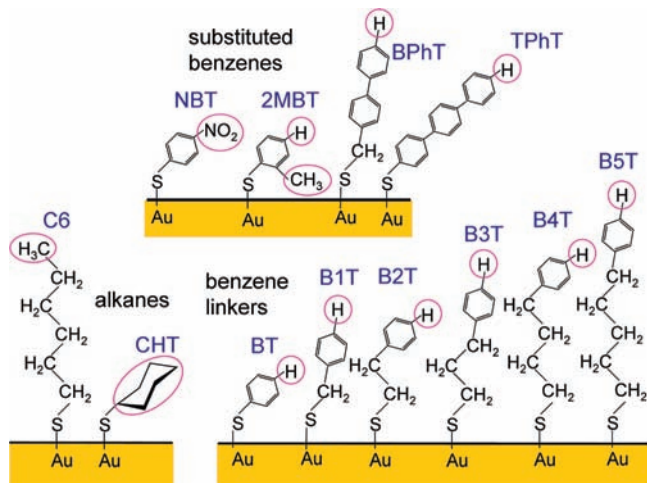


Figure 3. Structures and acronyms of individual molecules comprising the thiolate SAMs used in this study. The atomic moieties probed by SFG are indicated by circles.

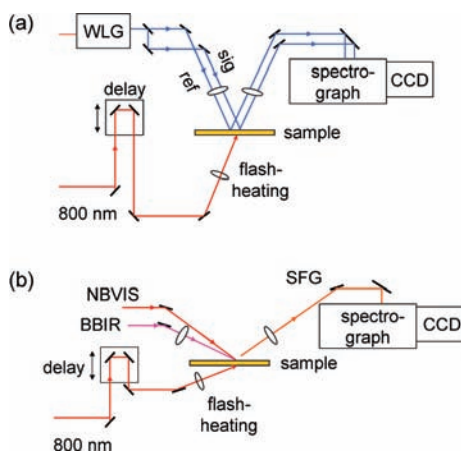


Figure 4. Schematics for flash-heating measurements with (a) white-light generation (WLG) reflectivity; (b) SFG. BBIR and NBVIS denote broadband femtosecond IR and narrow-band picosecond visible (800 nm) pulses.

without further purification. 4-Biphenylbenzenethiol (TPhT) was purchased from Frinton Laboratories and used without further purification. 4-Phenylbenzylthiol (BPhT) was synthesized starting with 4-phenyl benzyl alcohol (Chem-Impex, International, Inc.) following the procedures in ref 13 and ref 14. Phenylpropylthiol (B3T), phenylbutylthiol (B4T), and phenylpentylthiol (B5T) were synthesized from the corresponding bromides (TCI America, Co., Ltd.) using the procedure of ref 14.

B. Time-Dependent Reflectivity. The reflectivity measurements used the optical arrangement depicted in Figure 4a. A white-light continuum was generated in a 1 mm sapphire window and split into dual beams. The signal beam was reflected from a flash-heated region of the Au sample and the reference beam was reflected from a nearby region not flash-heated. The flash-heating conditions were comparable to what was used in the SAM measurements. The two probe beams were sent into a common imaging spectrograph with a CCD detector. We did not correct for time broadening due to chirp in the white light.

C. Flash Thermal Conductance. The details of these measurements were also described previously.^{1–3,12} As depicted in Figure 1a and Figure 4b, an 800 nm flash-heating pulse 130 fs in duration was incident on the back surface. The back surface is the side opposite the SAM, so the SAM was not exposed to the pulse's electric field. As discussed previously¹ and in section

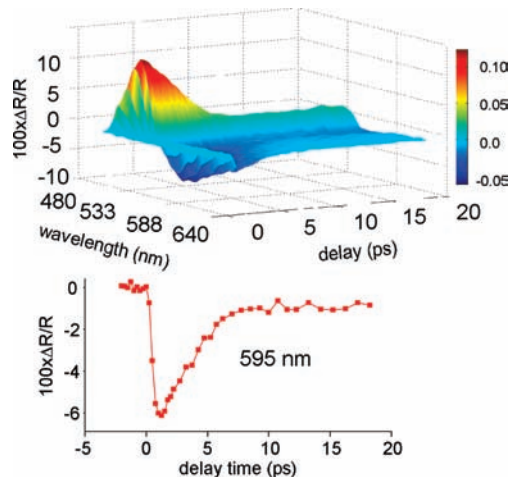


Figure 5. Time-dependence of Au reflectivity in the interband transition region after flash-heating to ~ 600 °C.

4A, heat is conducted very quickly from the back to the front surface. One difference from previous experiments is that the flash-heating pulse angle of incidence has been changed to 60° , rather than normal incidence, to match the probe pulses. This creates a chevron geometry between the pump and the probe pulses to eliminate geometrical transit time mismatches that could potentially degrade time resolution. The nominally circular laser beams then have an elliptical footprint on the sample with a 2:1 ($h:v$) aspect ratio. The flash-heating pulse energy needed to produce damaged spots on the Au surface that clearly had once been melted was about $100 \mu\text{J}$ for an elliptical spot with semi axes ($1/e^2$ intensity points) $700 \times 350 \mu\text{m}^2$ ($h \times v$). The flash-heating data were acquired using $60 \mu\text{J}$ pulses. Based on an Au melting temperature of 1064 °C, we estimate $\Delta T \approx 600$ K with $60 \mu\text{J}$ pulses. In previous work, we used a fluence that, with the present geometry, was the equivalent of $80 \mu\text{J}$ pulses, to generate an estimated $\Delta T \approx 800$ K.^{1–3,12} But after many thousands of pulses, the metal film developed faint damage tracks due to some unknown multiple-pulse interaction with the Au surface, and $60 \mu\text{J}$ pulses allowed for longer signal-averaging times.

The SFG probe consisted of femtosecond IR and picosecond “visible” (800 nm) pulses.¹⁵ In order to probe the central, more uniform region of the flash-heating volume, the IR pulses were $500 \times 250 \mu\text{m}^2$. The visible pulse was about 50% larger than the IR. The IR pulse duration was ~ 250 fs, and the visible pulses were time-asymmetric single-sided exponentials with 10.5 cm^{-1} fwhm and decay time constant 0.8 ps.¹⁶ The visible pulses were time delayed to suppress the nonresonant background from the Au surface, as discussed previously.^{12,16} The sample was mounted on a motorized positioner in continuous motion during data acquisition. An inert atmosphere purge was used to extend SAM lifetime, presumably by eliminating ozone. The SFG spectra were acquired with a 0.5 m spectrograph and CCD detector. The acquisition time for each spectrum depended on the intensity of SFG signal from each type of SAM, but was typically in the 4–10 s range.

3. Results

A. Time-Resolved Reflectivity. Time-dependent reflectivity spectra of a flash-heated Au surface are shown in Figure 5, encompassing the region of the 510 nm interband transition¹⁷ and regions where conduction (Drude) electrons dominate the reflectance. We show a typical slice of the data along time axis at 595 nm, in the Drude region. For a short time during and

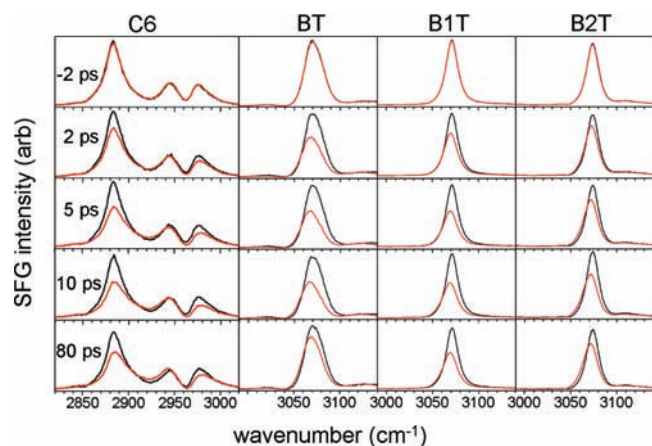


Figure 6. SFG spectra, at the indicated times after flash-heating to ~ 600 °C, for the terminal methyl CH stretch of C6 alkanethiol SAM on Au and the 4-position phenyl CH stretch of three benzenethiol SAMs on Au. The solid black curves are spectra taken with the SFG probe pulses preceding the flash-heating pulses.

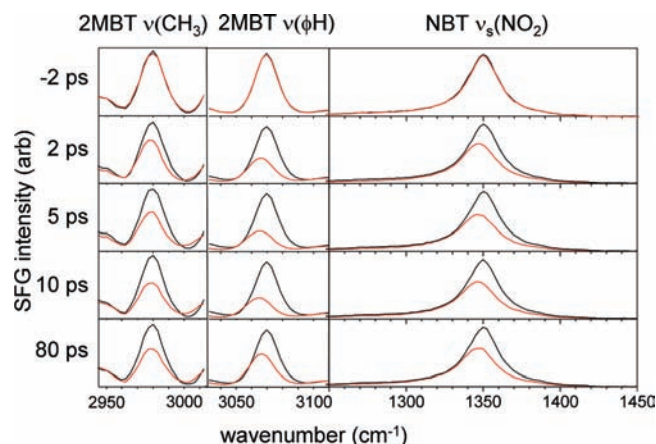


Figure 7. SFG spectra, at the indicated times after flash-heating to ~ 600 °C, for the methyl and phenyl CH stretch transitions of 2-methylbenzenethiolate SAM (2MBT) on Au and the symmetric nitro stretch of 4-nitrobenzenethiolate (NBT) SAM on Au. The solid black curves are spectra taken with the SFG probe pulses preceding the flash-heating pulses.

after the flash-heating pulses, due to excess hot electrons, the reflectivity change is as great as 6%. After the surface reaches thermal equilibrium at the higher temperature, at ~ 6 ps, the reflectivity change is about 1%. The time constant for thermalization is 2.5 ps. Note that this time constant is larger than reported previously,¹ where we observed the Au surface reaching 80% of the final temperature in 1 ps and 99% in 5 ps. The present data show 80% in 5 ps and 99% in 7 ps. Evidently, this is because our prior results involved a smaller T-jump^{1,2} of $\Delta T = 10$ K, whereas the present results were obtained with the same $\Delta T = 600$ K value used in SAM studies. The electron–phonon equilibration process slows down as ΔT increases as discussed in section 4A.

B. SFG Spectra. Because of the high symmetries or atomic arrangements of the molecular adsorbates depicted in Figure 3, in most cases, the SFG spectra arise from a single³ CH₃, CH, or NO₂ group. In Figure 3, we circled the moieties on each molecule deemed most responsible for the SFG spectrum.

Some representative SFG spectra using the nonresonant suppression technique,¹⁶ of SAMs with flash-heating to 600 °C, are shown in Figure 6 and Figure 7. In Figure 6, the C6 spectra derive from the terminal methyl groups and consist of three

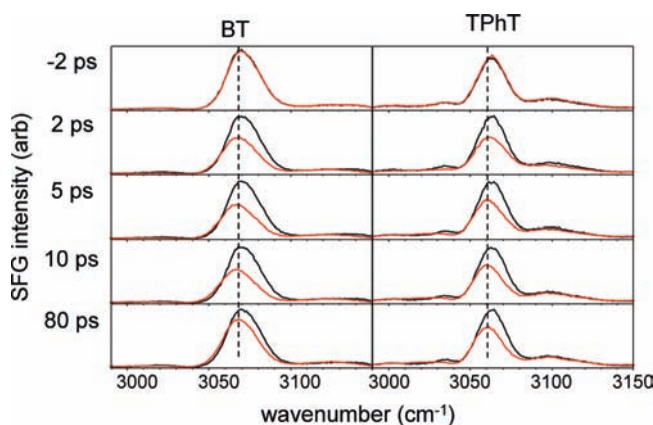


Figure 8. SFG spectra from flash-heated benzenethiol (BT) and terphenylthiol (TPhT) at indicated times after flash-heating. The solid black curves are spectra taken with the SFG probe pulses preceding the flash-heating pulses. Both SAMs evidence a thermal redshift. The BT SAM shows a redshift overshoot in the 2–10 ps time range, but the TPhT SAM shows no redshift overshoot.

peaks, representing the symmetric and antisymmetric methyl CH stretch and the Fermi resonance.¹⁸ Upon flash heating, all peaks lose intensity, but only the Fermi resonance shows a noticeable, but small, redshift.² The methylene transitions were too weak to be seen.

The CH-stretch transitions of BT, B1T, B2T, B3T, B4T, and B5T SAMs result from CH groups para to the thiolate linkage. The SFG hyperpolarizabilities of the CH groups at the 2 and 5 positions cancel each other, as do CH groups at the 3 and 6 positions. We know the SFG signal comes only from the para position because a CH₃ substituent at this position eliminates the aromatic CH-stretch signal.³ Upon flash-heating, the BT, B1T, and B2T CH-stretch transitions lose intensity and redshift slightly.

In the case of 2MBT, we simultaneously observed both methyl and phenyl CH-stretch transitions.¹⁹ The methyl signal comes solely from the methyl group, but because of the lower symmetry of the phenyl ring, we do not know if all of the phenyl CH-stretch signal comes solely from the 4-position CH group as in BT or B1T or whether the other CH groups also contribute. Figure 7 shows SFG spectra of 2MBT with improved data quality compared with ref 19. Both methyl and phenyl transitions lose intensity upon flash-heating, but the methyl transitions do not redshift. NBT, also shown in Figure 7, is the only SAM where we probed a transition other than C–H stretch. We probed both symmetric and asymmetric NO₂ stretching transitions. As illustrated by the $\nu_s(\text{NO}_2)$ data in Figure 7, both transitions lose intensity and redshift upon flash-heating.

In cyclohexanethiol (CHT), we probe two intense CH-stretch transitions. It is reported²⁰ that CHT at higher surface coverage exists predominantly in the equatorial chair conformer, so we are most probably seeing the result of two inequivalent CH sites, although we cannot rule out the possibility that we are seeing a mixed axial and equatorial chair SAM.

In the biphenyl (BPhT) and terphenyl (TPhT) SAMs, the SFG signal is believed, on the basis of our BT studies, to arise from the single CH moieties at the 8-position in BPhT and the 12-position in TPhT, as illustrated in Figure 3. Figure 8 compares SFG spectra from BT and TPhT. The vertical dashed lines are guides to the eye and they help illustrate that, while both BT and TPhT have thermal redshifts, BT has a redshift overshoot in the 2–10 ps range but TPhT has no redshift overshoot.

C. SFG Overshoot after Flash-Heating. Figures 9–11 show the time dependence after flash heating of the SFG

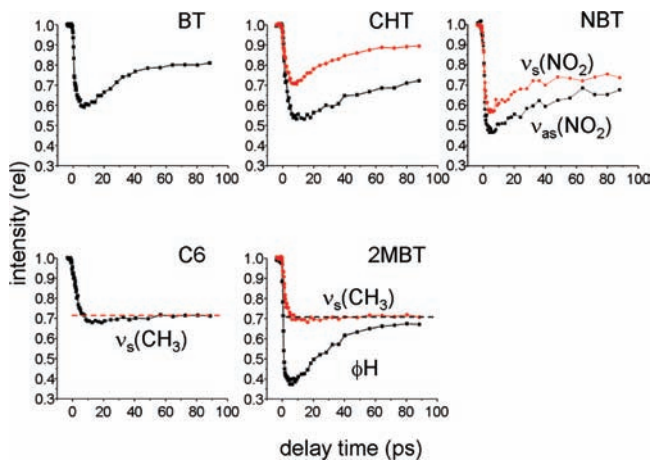


Figure 9. Time-dependence of SFG intensity loss for CH-stretch transitions of five SAM structures on Au. The dashed lines through the C6 and 2MBT data are guides to the eye to illustrate the small overshoots.

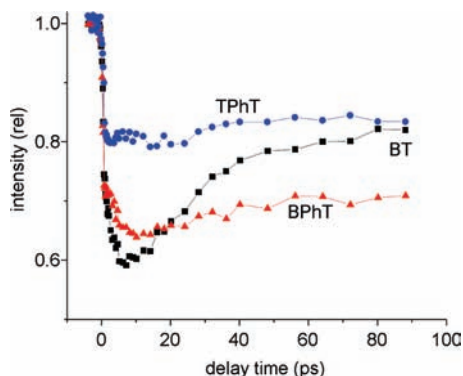


Figure 10. SFG intensity loss after flash heating of benzenethiol (BT), 4-phenyl benzylthiol (BPhT), and terphenyl thiol (TPhT). The large overshoot observed with BT is much smaller in the biphenyl and terphenyl thiols.

intensities (integrated spectral intensity) for several SAMs. In earlier studies of alkanethiols,^{1,2,19} we plotted these data as a “vibrational response function” for each SAM that was normalized to range from 0 to 1. This approach is not as helpful in comparing series of quite different molecular structures, because it conceals information about the magnitude of the SFG intensity drop, so here we will plot the fractional signal loss without further normalization.

To quantify the overshoot, we will use the value at long time minus the value at the SFG intensity minimum. Thus, for BT in Figure 9, the overshoot is 0.22. The BT overshoot decays with a time constant of 25 ps. In CHT, we observe two CH-stretch transitions associated with the two inequivalent hydrogen sites, and the overshoot is 0.2 in both cases. For NBT, the nitro-group overshoot is 0.2 for $\nu_{as}(\text{NO}_2)$, and possibly a bit less for $\nu_s(\text{NO}_2)$. The overshoot for C6 is 0.04. We did not notice this small overshoot in our earlier work² where the data were not as good. The longer (even-numbered) alkanes C8–C24 show no detectable overshoot. With 2MBT, the phenyl CH stretch shows a large overshoot of 0.28. The 2MBT methyl CH stretch might have an overshoot, but it is very small, 1–2% at most.

Figure 10 compares BT with BPhT and TPhT. Note the biphenyl compound has a methyl linker but BT and TPhT do not. The BT overshoot is 0.22; the BPhT overshoot is 0.05, and the TPhT overshoot is 0.02.

Figure 11 shows data for phenyl CH-stretch transitions of the benzene-linker molecules. The signal-to-noise ratio is best

for BT and B1T, and then it declines with increasing linker length. The SAMs with longer linkers seem to form less dense and less stable layers; so the signals are smaller, and we cannot signal average as long. The overshoot appears to decrease with increasing linker length (B4T is an exception), and there is no observable overshoot with B5T.

Figure 12 looks in more detail at the shorter-time behavior by comparing the normalized Au surface reflectance change to the normalized SFG intensity drop of BT and B5T. This format allows direct comparisons between the different types of measurements. The fast rise of the reflectance, with a 400 fs risetime (10%–90%), is due to hot electrons generated by the pulse, and this rise should be viewed as a representation of the laser apparatus response time. The time resolution stems from the finite duration of the heating pulse plus a small amount of wobble (tens of micrometers) of the sample translator. The BT SFG data has what can reasonably be termed a two-part rise, with the first part only marginally slower than the reflectance rise, and the second part characterized by a time constant in the 1.5–2.0 ps range. With the poor signal-to-noise ratio for B5T, it is not possible to definitively characterize the functional form of the rise in detail, but the B5T rise is clearly slower than the BT rise, most notably in the 1.5–4 ps range. If for comparison to BT we describe the B5T rise as having a faster initial part and a slower part, we would say the faster initial part was smaller than in BT and the slower part was slower than in BT.

D. SFG Thermometer. Prior to flash heating and at longer delay times, say $t > 50$ ps, the SAMs are in thermal equilibrium with the Au surface. The SFG intensities I_{SFG} at these times are representative of the surface temperature, and we will define an “SFG thermometer coefficient” Θ , the fractional change in I_{SFG} between an initial and final equilibrium temperature as

$$\Theta = \frac{\partial \ln I_{SFG}}{\partial T} \quad (1)$$

Looking at the data in Figures 9–11, the SAM with the largest thermometer coefficient is B1T. B1T SAMs also give relatively intense SFG signals, so of the SAMs in this study, B1T is the best SFG thermometer. Another excellent thermometer is BPhT, and in addition, the BPhT SAMs were the most stable with respect to long-term irradiation by laser pulses. Of course, because of the overshoot, B1T is not as useful as alkanethiol SAMs for studying shorter-time heat flow dynamics.

Figure 11 is suggestive of a chain alternation effect for Θ . The SAMs with 1, 3, and 5 carbon atoms in the linker are better thermometers than the SAMs with 0, 2, and 4 carbon atoms.

4. Discussion

In this section, we discuss a model for the overshoot, which involves pumping of SAM molecular vibrations by excited Au surface electrons. The SFG intensity loss overshoot is attributed to excitation of the probed vibrations by these electrons. The SFG redshift overshoot is attributed to electron excitation of at least some of the lower-energy vibrations, that are anharmonically coupled to the probed vibrations, to occupation numbers that temporarily exceed their ultimate populations in equilibrium at the higher temperature. We will now discuss the flash-heating process, electron excitation of SAM molecule vibrations, its effects on the SFG signal intensity and redshift, and the dependence of the electron excitation process on distance above the surface.

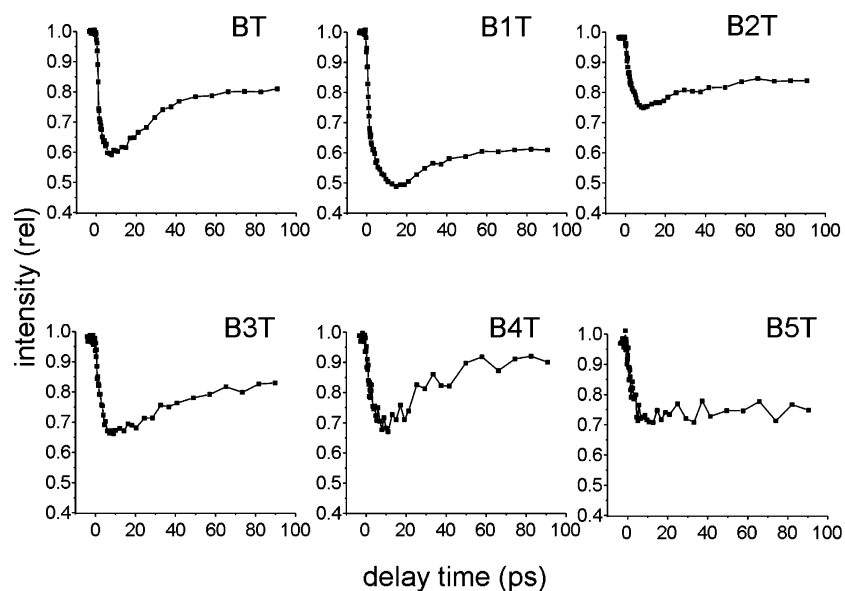


Figure 11. Time-dependence of SFG intensity loss for phenyl-CH stretch of six SAM structures where a phenyl group is attached to the thiolate by the indicated number of $-\text{CH}_2-$ linkers. As the linker becomes longer, the overshoot becomes less prominent.

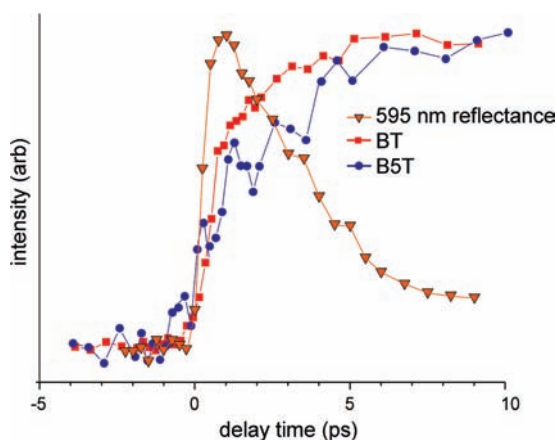


Figure 12. Comparison of the flash-heating induced shorter-time rise of the Au reflectance at 595 nm, and the SFG signals (normalized) from benzenethiol (BT) and benzene-pentyl thiol (B5T) SAMs on Au.

A. Femtosecond Laser Heating. Femtosecond near-IR laser heating of Au is frequently described by a “two-temperature” model.^{21–24} With small ΔT of a few Kelvin, the laser pulses excite a small fraction of the conduction electrons, which thermalize in a few femtoseconds through electron–electron interactions.^{21,23,25} The hot electrons have a high mobility,^{23,26} so they efficiently transport heat from the pumped (back) side of the Au layer to the front side. The initial electron temperature T_e is much greater than ΔT , because the electronic heat capacity is a small fraction of the total heat capacity. The hot electrons cool because of electron–phonon coupling as the lattice heats up, and an equilibrium ΔT is achieved in about 1 ps.²⁶

Larger-amplitude heating of Au has been studied in the context of femtosecond laser melting,²⁷ laser ablation,²⁸ and plasma generation (“warm dense matter”).^{29,30} The melting studies are most relevant here. In order to create a T-jump of hundreds of Kelvin, it is necessary to excite a larger fraction of the conduction electrons, including some of the d -band electrons. Interactions between conduction electrons and between electrons and d -band holes retard the electron–lattice equilibration.^{31,32} Under the flash-heating conditions used here, according to the “improved” model of Jiang and Tsai,²⁴ the electron temperature

should initially reach a peak of $T_e \approx 2 \times 10^4$ K and the equilibration time should be ~ 5 ps.

Our Au reflectivity data in Figure 5 show that the lattice heats up in ~ 5 ps. This result is in good agreement with the predictions mentioned above and with the electron diffraction study of Au melting by Dwyer et al.²⁷

Figure 12 compares the shorter-time Au surface reflectivity on bare Au and SFG transients from BT and B5T. These data show that the SFG signal loss associated with the overshoot effect occurs in the 0–0.6 ps time range. This 0.6 ps process is associated with the 400 fs risetime characterizing the apparatus response, as opposed to the 2.5 ps hot electron decay/lattice heating, the ~ 20 ps decay of vibrational excitations, or the microsecond dissipation of the surface high temperature. Thus, we conclude that the overshoot results from a process that occurs primarily during the flash-heating pulse. We note that the back side heating geometry ensures that the SAM molecules never directly see light from the flash-heating pulse, so the overshoot is associated with energetic electrons present only during the pulse. We cannot discount the possibility that a smaller part of the overshoot might result from the hottest electrons present immediately after the pulse. However, it could only be the hottest electrons, since the cooler (but still very hot) electrons present at, for example, 1–4 ps after the pulse, appear not to significantly contribute to the SFG overshoot. We also note that, in experiments on BT where we attenuated the flash-heating pulses to produce one-half the T-jump ordinarily used, the relative magnitudes of overshoot and thermometer effect were unchanged. This showed the electrons responsible for the overshoot were not created by a multiphoton interaction.

B. Vibrational Excitations Generated by Au Electrons.

Although the overshoot stems primarily from effects of hot electrons present during the flash-heating pulses, the data at hand do not provide much insight into the actual mechanism of vibrational heating. In this section, we briefly speculate on some possibilities, described as “incoherent” or “coherent” excitation processes, as motivation for future studies.

On the basis of many studies of laser desorption of molecules from metal surfaces, it is well-known that hot electrons generated by laser pulses incident on a metal surface can create adsorbate vibrational excitations.^{21,33,34} The mechanism, in which

incoherent electrons pump energy into adsorbates, is usually described as involving electron tunneling to the adsorbate, to temporarily form an anion. The anionic states decay rapidly because of strong electrostatic coupling with the metal substrate through image charges. For C_6F_6 on Cu(111), the anionic resonance lives for ~ 7 fs,³⁵ and we might expect similar lifetimes for the SAMs studied here. These anions would not be detectable in our experiments using 100s of femtosecond pulses. Creation and destruction of anionic states can excite vibrations of the adsorbate molecules through Franck–Condon overlap.

An intense oscillating field will also drive plasma excitations of a metal layer, which are coherent electron oscillations in the plane. The coherent electron oscillations will not persist after the flash-heating pulses, because of the large damping constants. While the electrons are coherently driven, the oscillating electric field near the surface could create excitations in modes having dipole moments parallel to the surface. Thus, the two broad classes of electron heating mechanisms might be distinguished via differing selection rules.

C. Effects of Hot Electrons on SFG Spectral Intensities.

In our proposed model, overshoot of the SFG intensity loss is associated with surface electron excitation of the probed CH stretch (or NO_2 stretch). The probed vibrations are high enough in frequency that they would otherwise never be significantly populated thermally by the flash-heated Au(111) surface. The remainder of the SFG intensity loss, the part associated with the molecular thermometer, is attributed to thermally induced molecular disordering, as in our earlier alkanethiol^{1,2} studies.

SFG is sensitive to both surface order³⁶ and vibrational population.^{37,38} As the surface order decreases, the SFG intensity decreases with an asymptotic limit of zero for an isotropic system. SFG signals also lose intensity when the probed state becomes vibrationally excited. Both these effects are apparent in the following frequency-domain formulation of SFG.³⁶

$$I_{ijk,SFG} \propto |P_i^{(2)}| \propto |(N_g - N_e) \cdot \sum_{abc} \langle (a \cdot i)(b \cdot j)(c \cdot k) \rangle \beta_{abc} E_j(\omega_{VIS}) E_k(\omega_{IR})|^2 \quad (2)$$

Equation 2 describes the i th polarization component of the SFG intensity I_{ijk} created by the $E_j(\omega_{VIS})$ and $E_k(\omega_{IR})$ local electric fields. N_g and N_e are the number density of molecules in the vibrational ground and first excited state; $a \cdot i$ is the projection of the a th unit vector in the molecular reference frame onto the i th unit vector in the surface frame; $\langle \dots \rangle$ is the orientational ensemble average, and β_{abc} is the molecular hyperpolarizability in the molecular frame.

The SFG intensity can also be affected by time-varying Fresnel coefficients that change both the local electric fields $E_j(\omega_{VIS})$ and $E_k(\omega_{IR})$ and the reflected SFG signal field. The flash-heating pulse undoubtedly changes the optical properties of the gold substrate as seen in the reflectivity data. Mechanical processes such as thermal lensing or thermal deflection occur far too slowly to account for the faster transients we observe. The possibility that the faster parts of the SFG intensity drop result from changes in the substrate optical properties is inconsistent with our results. Looking at the reflectance data near 640 nm, which is close to the SFG signal for our experiments, the reflectivity drops by a maximum of $\sim 5\%$. If we look further away from the interband transition region toward the probe pulses, where the optical properties are dictated by the conduction electrons or Drude electrons, the pump-induced

changes are even smaller. The BT and B1T SFG signals, however, decrease by $\sim 50\%$ within the first picosecond. Furthermore, if the time dependence of the substrate optical properties was significantly imparted to the SFG signals, then C6 would also exhibit an abrupt loss of SFG intensity similar to that of the benzenethiols, and this was not observed. Undoubtedly, the substrate reflectivity changes do contribute to the SFG transients, but the effects are overwhelmed by thermally induced SAM disordering and vibrational excitation of the probed modes.

It is interesting that the amount of vibrational excitation needed to produce the observed overshoot is rather small. The benzene CH stretch $\nu = 1 \rightarrow 2$ transition is red shifted³⁹ by 122 cm^{-1} from the fundamental transition. In this limit of large anharmonic shift, the SFG signal loss is proportional to $(1 - 2\Delta n)^2$,³⁸ where Δn is the fraction of excited states. In BT, a case of relatively large overshoot, the overshoot of ~ 0.2 corresponds to 5% CH-stretch excitation.

Since the overshoot is caused by electron pumping of the probed CH stretch, the time constant for overshoot decay should be associated with the vibrational T_1 of the CH stretch. It is difficult to extract a precise time constant for T_1 in cases where the overshoot is small. According to our model, decay of the overshoot corresponds to the vibrational lifetime $T_1/2$, and the data suggests a lifetime $T_1 \approx 25$ ps for BT and B1T. The vibrational T_1 's for CHT and NBT seem a bit longer, in the 40 ps range, but otherwise, all of the other SAMs seem to have T_1 in the 25 ps neighborhood. We note that it is difficult to study vibrational relaxation of higher frequency modes of adsorbates on metal surfaces, because if one tries to use an IR laser pulse to excite the vibration, the surface is flash-heated and the heat flow from surface to adsorbate is a bigger effect than heat flow from adsorbate to surface. This issue does not arise with dielectric surfaces, for instance, CO on salt.⁴⁰ It is interesting that the observed time constant of 25 ps is quite a bit longer than the 6 ps relaxation of CH-stretch excitations in liquid benzene.⁴¹

D. 2-Methyl Benzenethiol. The 2MBT SAM is an especially interesting case since we simultaneously probe two different parts of the molecules, the phenyl ring and the methyl substituent, and they have clearly different responses to flash heating as seen in Figure 9. We discussed this data previously,³ but the improved quality of the present data permit a more in-depth analysis. Let us operate from the premise that the methyl CH-stretch SFG signal, which shows no overshoot, is a molecular thermometer of the alkanethiol type, and its time response is sensitive solely to disordering of the SAM layer, whereas the phenyl CH-stretch signal is sensitive to both disordering and an excited-state population created by electron excitation.

Equation 2 then shows that, if we divide the 2MBT phenyl signal by the 2MBT methyl signal and take the square root, we will obtain a function that is proportional to the time-dependent vibrational population difference $\Delta n = N_g - N_e$, which as seen in Figure 13 has an instantaneous rise. This rise confirms the view that vibrational excitations of the higher-frequency transition probed by SFG are created during the flash-heating laser pulses. The decay in Figure 13 has the ~ 25 ps time constant associated with the vibrational T_1 of these excitations.

The risetime of the 2MBT methyl data in Figure 9 results from thermal disordering, which itself depends on the rate of heat flow into the SAM and the response time for a hot SAM to become disordered. In earlier works, we argued on the basis of T-jump molecular simulations, that the SAM response time

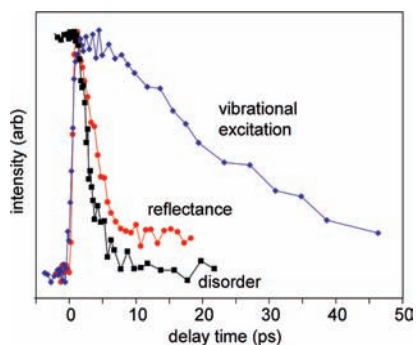


Figure 13. From the 2-methyl benzenethiol (2MBT) data in Figure 9, we used eq 2 to compute the vibrational excitation of the phenyl CH stretch (blue diamonds). A comparison to the Au surface reflectance data (red circles) shows these vibrational excitations were created only during the reflectance rise, which represents the laser time response, so they must be excited by hot nonthermal electrons generated during the flash-heating pulses. The 2MBT methyl signal corresponds to the time for SAM thermal disordering. The disordering is slightly faster than the reflectance decay. The reflectance decay approximately corresponds to the rate of heating the Au lattice to the final temperature.

was ~ 0.5 ps,^{1,2} in other words, that the SFG thermometer had a response time of 0.5 ps. Thus, any significantly longer time constants should be associated with heat flow rather than thermometer intrinsic response. In Figure 13, we have plotted the square root of the methyl SFG data. The time dependence can be fit by an exponential function with a time constant of 3 ps, which we interpret as the time for SAM disordering. This time constant should be regarded as more accurate than the one given previously.³ As shown in Figure 13, the disordering process is slightly faster than the decay of the reflectance data, which reflects the time for Au surface phonons to heat up.

This odd-seeming result, that the SAM disorders somewhat faster than the surface attains the final temperature of ~ 600 °C, is in good agreement with and is explained by our alkanethiol simulations.^{1,2} The simulations showed that above ~ 300 °C the alkanethiol disorder stopped increasing. The BT SAM disorder will also likely saturate at a similar temperature. Thus, the time constant for the SAM to disorder is approximately the time for the surface temperature to rise from ambient to 300 °C, which is slightly faster than the time for the surface to reach ~ 600 °C.

E. Distance Dependence of Electron Excitation. Several observations show that the likelihood of vibrational excitation by surface electrons becomes small for moieties connected to the surface by 4–6 or more carbon atoms. First, the overshoot becomes minimal for alkanes C6 and longer. Second, the overshoot is minimal for benzenes spaced 5 carbon atoms (BPeT) from the surface.

The results for substituted benzenes raise some interesting questions that could form the basis for further investigations. In the phenyl, biphenyl, and terphenyl series, the overshoot decreases with increasing distance from the Au surface as with the benzene-linker molecules. The overshoot is large for the nitro transitions of NBT, which seems reasonable since the nitro π electrons are part of the coupled aromatic π -electron system. Electron tunneling onto the coupled phenyl-nitro orbitals would be expected to generate vibrational excitations of both moieties.

An interesting case is the methyl substituent in 2MBT, which shows no overshoot. This methyl group is close to the Au surface (Figure 3), viewed either in physical space or by the spacing in units of carbon atoms. This puzzling observation is suggestive of the possibility that electron heating of the methyl

CH-stretch vibrations is forbidden by a selection rule, which might provide a method to decide between the incoherent and the coherent pumping mechanisms mentioned above. In the coherent pumping mechanism, excitations are generated by electrons oscillating in the plane of the metal surface, so excitation would be inefficient when the dipole moment is perpendicular to the plane, which is the case for the methyl group of 2MBT. (The C_{3v} axis of the methyl group is parallel to the plane so the asymmetric stretch dipole moment is perpendicular to the plane). Thus, the 2MBT results seem to support the coherent electron heating mechanism.

F. Heating by Surface Electrons Is a Small Effect Overall.

In this section we show that, compared with the heat supplied by the Au lattice, the energy supplied to the SAM by surface electrons is small. In the case of the vibrations directly probed by SFG, we have a direct measure of the level of electron excitation. Above, we showed that, in one of the more dramatic cases, the large overshoot of BT, hot electrons created a maximum of 5% excitation of the probed CH stretch (3070 cm^{-1}). This corresponds to 150 cm^{-1} per molecule of the SAM or 1.8 kJ M^{-1} . By taking the heat capacity C_p of benzene to be 135 $\text{J M}^{-1} \text{K}^{-1}$, the electron-excited CH stretch accounts for just 13 K of the ~ 600 K temperature rise. So the heat deposited into the probed vibration by electron excitation is quite small, even though the effects of electron excitation on the SFG intensity are not small.

Most of the vibrational transitions are not monitored by SFG, so in order to understand how much energy is in these unobserved transitions, we will look at cases where SAMs consist of a “base” region close to Au where we know electron excitation is substantial and a probed region away from the base. The two best examples are the C16 chains, where the base consists of the first few carbon atoms and the probe is located at the terminal methyl group, and TPhT where the base is BT and the probe is located at the para position of the third phenyl ring (Figure 3).

In the C16 chains, if electron heating of the base involved a significant amount of energy transfer from the Au surface, we would see the effects of a burst of energy traveling along the chain to the terminal methyl groups. The electron-excited vibrations become excited within ~ 500 fs. The transit time from the base to the methyl terminus of a C16 chain is ~ 1 ps.² So if the hot surface electrons contributed a substantial fraction of the total heat in the SAM, there would be a significant SFG intensity loss by 2 ps, which Figure 1b shows there is not.

In the TPhT case, we look at the redshift overshoot. The BT base clearly shows a redshift overshoot (Figure 2 and Figure 8). The redshift results from excitation of lower-energy vibrations anharmonically coupled to the probed CH-stretch transition, most likely ring and CH deformation modes in the 500 – 1500 cm^{-1} range. Now, we can imagine two limiting cases. In the first case, electron heating is a large effect, so that the redshift is due to electron excitation of all the vibrations in this range to levels that temporarily correspond to temperatures even greater than 600 °C. In the second case, electron heating is a small effect, and electrons are simply exciting a few vibrations that are well-coupled to the probed CH stretch, to produce the redshift overshoot. If the first case were correct, in the TPhT measurements, this very large amount of energy in the BT base would very quickly rush into the other phenyl rings, and we would see a substantial redshift overshoot in TPhT, which we do not (Figure 8). Therefore, our data support the second case where electron excitation of the unobserved vibrations is small compared with phonon excitation. One reasonable scenario is

that the BT redshift overshoot results from electrons generating 5–10% excitation of 5–10 lower-energy (500–1500 cm^{-1}) vibrations of BT that have large cross sections for either the coherent or incoherent electron heating mechanisms and relatively strong anharmonic coupling to the probed vibration. In this event, the total energy delivered to unobserved vibrations with an average energy of 1000 cm^{-1} would be a few hundred cm^{-1} , leading to a few tens of Kelvin temperature increase.

5. Summary and Conclusions

In order to better understand energy transfer from flash-heated Au surfaces to thiolate SAMs, we have extended our prior flash-thermal calorimetry studies of C6–C24 alkanes to SAMs having probed groups closer to the Au surface. We also performed new time-resolved reflectivity studies of Au under the same conditions used for the SAM studies. Finally, we probed substituent sites on aromatic SAMs.

The aromatic BT (Figure 2) evidenced a significant overshoot in the CH-stretch SFG intensity loss and a much smaller overshoot in the CH-stretch peak redshift. The intensity overshoot phenomenon is not limited to aromatic SAMs, since we see it in cyclohexanethiol and in the shortest alkanethiol that we can study, C6. The time dependence of the overshoot shows that it results from Au excited electrons present only during the ~ 300 fs flash-heating pulses. The SFG intensity loss is consistent with a proposed mechanism where these hot electrons directly excite the CH-stretch transition being probed. The overshoot decay represents relaxation of this excess vibrational energy. Because of the high sensitivity of SFG intensity loss to vibrational excitation, no more than a few percent of the SAM molecules need CH-stretch vibrational excitations to account for even the largest observed overshoots. The redshift overshoot is associated with hot electron excitation of lower energy vibrations that are anharmonically coupled to the probed vibration.

The studies with benzene-linker molecules indicate that surface electron excitation of SAM vibrations becomes inefficient when the probed groups are set off from the Au surface by a distance in the range of 4–6 carbon atoms. This view is also supported by our alkanethiol studies, where only the shortest C6 alkanethiol evidenced any overshoot at all.

Several observations show that, compared with the heat supplied by the Au lattice, the energy supplied to the SAM by the surface electrons is small. The amount of energy transferred to the probed CH-stretch transitions can account for only ~ 10 K of the total ~ 600 K T-jump. Electron excitation of the vibrations not observed appears also to be an effect of similar magnitude, as deduced from studies of molecules such as C16 and TPhT which can be viewed as having a base region that is excited by surface hot electrons on the 400 fs time scale and a probe region located several carbon atoms downstream which does not see a large energy burst from the base on the relevant time scale.

The results shown in Figure 1c,d indicated that heat transfer from Au to alkanethiol SAMs occurred initially to a 0.8 nm “base region” 4–5 carbon atoms in length. The new results presented here also indicate that SAM heating by surface electrons also has a similar 4–5 carbon atom length scale. However, we have now shown that phonon heating is the dominant heat transfer mechanism, since the total energy transfer from hot electrons is small. Therefore, the base region we observed previously refers to phonon heating. It seems as if the similar 4–5 carbon atom length scale for transfer from the surface to the SAM for both electron and lattice heating might simply be a coincidence.

Energy transferred by hot surface electrons directly to probed vibrations of functional groups lying close to the Au surface has a disproportionately large effect on the SFG signal for the first few tens of picoseconds. Thus, in SAMs evidencing large overshoots on the <30 ps time scale, the SFG signal is not a good molecular thermometer. Although the electron heating process hinders the study of ultrafast heat flow in SAMs, it is useful for creating nonthermal vibrational populations in SAMs whose relaxation processes can be investigated. However, since we are primarily interested in heat flow, we want to look for systems such as the alkane chains, where short-time heat flow is directly reflected in the SFG signal. In this regard, the 2MBT and TPhT molecules are very interesting, since there is little or no overshoot when probing the CH_3 substituent of 2MBT or the terminal phenyl group of the terphenyl moiety. Thus, it appears that alkyl-substituted phenyl SAMs or polyphenyl SAMs will be good systems to understand heat flow in molecule wires that incorporate aromatic⁷ moieties.

Acknowledgment. This material is based upon work supported by the National Science Foundation under Award No. DMR 0955259, the Air Force Office of Scientific Research under Award No. FA9550-09-1-0163, and the Army Research Office under Award Nos. W911NF-05-1-0266 and W911NF-09-1-0238. We thank the Center for Microanalysis of Materials at the University of Illinois at Urbana–Champaign, supported by Award No. DEFG02-91ER45439. J.A.C. was supported in part by a fellowship from Merck Research Laboratories.

References and Notes

- (1) Wang, Z.; Cahill, D. G.; Carter, J. A.; Koh, Y. K.; Lagutchev, A.; Seong, N.-H.; Dlott, D. D. *Chem. Phys.* **2008**, *350*, 31.
- (2) Wang, Z.; Carter, J. A.; Lagutchev, A.; Koh, Y. K.; Seong, N.-H.; Cahill, D. G.; Dlott, D. D. *Science* **2007**, *317*, 787.
- (3) Carter, J. A.; Wang, Z.; Dlott, D. D. *J. Phys. Chem. A* **2008**, *112*, 3523.
- (4) Cahill, D. G.; Ford, W. K.; Goodson, K. E.; Mahan, G. D.; Majumdar, A.; Maris, H. J.; Merlin, R.; Phillpot, S. R. *J. Appl. Phys.* **2003**, *93*, 793.
- (5) Segal, D.; Nitzan, A. *J. Chem. Phys.* **2002**, *117*, 3915.
- (6) Segal, D.; Nitzan, A.; Hänggi, P. *J. Chem. Phys.* **2003**, *119*, 6840.
- (7) Galperin, M.; Ratner, M. A.; Nitzan, A. *J. Phys.: Condens. Matter* **2007**, *19*, 103201.
- (8) Nitzan, A. *Science* **2007**, *317*, 759.
- (9) Ge, Z.; Cahill, D. G.; Braun, P. V. *J. Phys. Chem. B* **2004**, *108*, 18870.
- (10) Ge, Z. B.; Cahill, D. G.; Braun, P. V. *Phys. Rev. Lett.* **2006**, *96*, 186101.
- (11) Wang, R. Y.; Segalman, R. A.; Majumdar, A. *Appl. Phys. Lett.* **2006**, *89*, 173113.
- (12) Carter, J. A.; Wang, Z.; Dlott, D. D. *Acc. Chem. Res.* **2009**, *42*, 1343.
- (13) Tongkate, P.; Pluempunapat, W.; Chavasiri, W. *Tetrahedron Lett.* **2007**, *49*, 1146.
- (14) Han, C.-C.; Balakumar, R. *Tetrahedron Lett.* **2006**, *47*, 8255.
- (15) Patterson, J. E.; Lagutchev, A. S.; Huang, W.; Dlott, D. D. *Phys. Rev. Lett.* **2005**, *94*, 015501.
- (16) Lagutchev, A.; Hambir, S. A.; Dlott, D. D. *J. Phys. Chem. C* **2007**, *111*, 13645.
- (17) Scouler, W. J. *Phys. Rev. Lett.* **1967**, *18*, 445.
- (18) Harris, A. L.; Chidsey, C. E. D.; Levinos, N. J.; Loiacono, D. N. *Chem. Phys. Lett.* **1987**, *141*, 350.
- (19) Carter, J. A.; Wang, Z.; Dlott, D. D. Watching vibrational energy in molecules with high time and space resolution. In *Proceedings of the XXIst International Conference on Raman Spectroscopy*; Withnall, R., Chowdhry, B. Z., Eds.; IM Publications LLP: Charlton, Chichester, 2008; p 112.
- (20) Joo, S.-W.; Chung, H.; Kim, K.; Noh, J. *Surf. Sci.* **2007**, *601*, 3196.
- (21) Frischkorn, C.; Wolf, M. *Chem. Rev.* **2006**, *106*, 4207.
- (22) Groeneveld, R. H. M.; Sprik, R.; Lagendijk, A. *Phys. Rev. B* **1992**, *45*.
- (23) Juhasz, T.; Elsayed-Ali, H. E.; Smith, G. O.; Suárez, C.; Bron, W. E. *Phys. Rev. B* **1993**, *48*.
- (24) Jiang, L.; Tsai, H.-L. *J. Heat Transfer* **2005**, *127*, 1167.

- (25) Zhigilei, L. V.; Leveugle, E.; Garrison, B. J. *Chem. Rev.* **2003**, *103*, 321.
- (26) Brorson, S. D.; Fujimoto, J. G.; Ippen, E. P. *Phys. Rev. Lett.* **1987**, *59*, 1962.
- (27) Dwyer, J. R.; Jordan, R. E.; Hebeisen, C. T.; Harb, M.; Ernstorfer, R.; Dartigalongue, T.; Miller, R. J. D. *J. Mod. Opt.* **2007**, *54*, 905.
- (28) Zhigilei, L. V.; Garrison, B. J. *Proc. SPIE Int. Soc. Opt. Eng.* **1998**, *3254*, 135.
- (29) Ping, Y.; Hanson, D.; Koslow, I.; Ogitsu, T.; Prendergast, D.; Schwegler, E.; Collins, G.; Ng, A. *Phys. Rev. Lett.* **2006**, *96*, 255003.
- (30) Ernstorfer, R.; Harb, M.; Hebeisen, C. T.; Sciaini, G.; Dartigalongue, T.; Miller, R. J. D. *Science* **2009**, *323*, 1033.
- (31) Hu, M.; Petrova, H.; Hartland, G. V. *Chem. Phys. Lett.* **2004**, *391*, 220.
- (32) Chan, W.-L.; Averback, R. S.; Cahill, D. G.; Ashkenazy, Y. *unpublished* **2009**, *102*, 095701.
- (33) Antoniewicz, P. R. *Phys. Rev. B* **1980**, *21*.
- (34) Franchy, R. *Rep. Prog. Phys.* **1998**, *61*, 691.
- (35) Vondrak, T.; Zhu, X.-Y. *J. Phys. Chem. B* **1999**, *103*, 3449.
- (36) Shen, Y. R. *The Principles of Nonlinear Optics*; Wiley: New York, 1984.
- (37) Bredenbeck, J.; Ghosh, A.; Smits, M.; Bonn, M. *J. Am. Chem. Soc.* **2008**, *130*, 2152.
- (38) Ghosh, A.; Smits, M.; Sovago, M.; Bredenbeck, J.; Müller, M.; Bonn, M. *Chem. Phys.* **2008**, *350*, 23.
- (39) Reddy, K. V.; Heller, D. F.; Berry, M. J. *J. Chem. Phys.* **1982**, *76*, 2814.
- (40) Ewing, G. E. *Acc. Chem. Res.* **1992**, *25*, 292.
- (41) Seong, N.-H.; Fang, Y.; Dlott, D. D. *J. Phys. Chem. A* **2009**, *113*, 1445.

JP906082U